AIP Advances

Improving the efficiency of copper indium gallium (Di-)selenide (CIGS) solar cells through integration of a moth-eye textured resist with a refractive index similar to aluminum doped zinc oxide

M. Burghoorn, B. Kniknie, J. van Deelen, M. Xu, Z. Vroon, R. van Ee, R. van de Belt, and P. Buskens

Citation: AIP Advances **4**, 127154 (2014); doi: 10.1063/1.4905456
View online: http://dx.doi.org/10.1063/1.4905456
View Table of Contents: http://scitation.aip.org/content/aip/journal/adva/4/12?ver=pdfcov
Published by the AIP Publishing

Improving the efficiency of copper indium gallium (Di-)selenide (CIGS) solar cells through integration of a moth-eye textured resist with a refractive index similar to aluminum doped zinc oxide

M. Burghoorn,[1] B. Kniknie,[1] J. van Deelen,[1] M. Xu,[1,2] Z. Vroon,[1,3] R. van Ee,[1] R. van de Belt,[4] and P. Buskens[1,5,a]

[1]*The Netherlands Organisation for Applied Scientific Research (TNO), De Rondom 1, 5612 AP, Eindhoven, The Netherlands*
[2]*Delft University of Technology, Optics Group, Van der Waalsweg 8, 2628 CH, Delft, The Netherlands*
[3]*Zuyd Hogeschool, Nieuw Eyckholt 300, 6419 DJ, Heerlen, The Netherlands*
[4]*Kriya Materials BV, Urmonderbaan 22, 6167 RD, Geleen, The Netherlands*
[5]*DWI – Leibniz Institute for Interactive Materials, Forckenbeckstrasse 50, 52056, Aachen, Germany*

(Received 17 October 2014; accepted 19 December 2014; published online 31 December 2014)

Textured transparent conductors are widely used in thin-film silicon solar cells. They lower the reflectivity at interfaces between different layers in the cell and/or cause an increase in the path length of photons in the Si absorber layer, which both result in an increase in the number of absorbed photons and, consequently, an increase in short-circuit current density (J_{sc}) and cell efficiency. Through optical simulations, we recently obtained strong indications that texturing of the transparent conductor in copper indium gallium (di-)selenide (CIGS) solar cells is also optically advantageous. Here, we experimentally demonstrate that the J_{sc} and efficiency of CIGS solar cells with an absorber layer thickness (d_{CIGS}) of 0.85 μm, 1.00 μm and 2.00 μm increase through application of a moth-eye textured resist with a refractive index that is sufficiently similar to AZO (n_{resist} = 1.792 *vs.* n_{AZO} = 1.913 at 633 nm) to avoid large optical losses at the resist-AZO interface. On average, J_{sc} increases by 7.2%, which matches the average reduction in reflection of 7.0%. The average relative increase in efficiency is slightly lower (6.0%). No trend towards a larger relative increase in J_{sc} with decreasing d_{CIGS} was observed. *Ergo*, the increase in J_{sc} can be fully explained by the reduction in reflection, and we did not observe any increase in J_{sc} based on an increased photon path length. [http://dx.doi.org/10.1063/1.4905456]

INTRODUCTION

Textured transparent conductors are widely used in thin-film silicon solar cells.[1–3] A large number of studies on this subject matter have been reported, focusing both on randomly and periodically textured surfaces.[4,5] Since thin-film Si cells are manufactured through sequential deposition of the cell layers on the cover glass plate coated with the transparent conductor, the texture of the conductor may (partially) replicate in the other cell layers, resulting in roughened interfaces between the different layers of the solar cell.[6] It has been reported that this roughness can lower the reflectivity at interfaces between different layers, resulting in a larger amount of photons that penetrate into the active layer.[7] Additionally, the roughness at the interface may lead to an increased

[a]Author to whom correspondence should be addressed. Electronic mail: pascal.buskens@tno.nl; buskens@dwi.rwth-aachen.de

path length of photons in the Si absorber layer, resulting in an increase of absorption.[8] Hence, the efficiency of thin-film Si cells typically increases by about 25% through use of a textured transparent conductor as compared to a flat conductor.[3]

Copper indium gallium (di-)selenide (CIGS) solar cells are produced by sequential deposition of the required layers on the substrate.[9] First, the conductive back contact – typically Mo – is deposited, followed by the CIGS absorber layer, the buffer layer, typically CdS, a layer of intrinsic zinc oxide and the transparent conductor, mostly aluminum doped zinc oxide (AZO). Hence, a potential texture on the surface of the transparent conductor would not be replicated at the interfaces between other cell layers. Nonetheless, through optical simulations we recently obtained strong indications that texturing of the surface of the transparent conductor would be optically advantageous.[10]

Instead of direct texturing of the AZO layer, we applied a transparent UV curable resist with a refractive index sufficiently similar to AZO to avoid large optical losses at the resist-AZO interface (n_{resist} = 1.792 *vs.* n_{AZO} = 1.913 at 633 nm), which is suitable for texturing with UV nano-imprint lithography (NIL). In that way, the two-layered stack AZO-textured resist optically resembles textured AZO, and we can apply well-defined textures without performing tedious experimental studies on texturing of AZO, *e.g.* through chemical etching. Here, we experimentally demonstrate that the short-circuit current density (J_{sc}) and efficiency of CIGS solar cells with a CIGS layer thickness (d_{CIGS}) of 0.85 μm, 1.00 μm and 2.00 μm increase through application of a moth-eye textured resist with a refractive index sufficiently similar to AZO to avoid large optical losses at the resist-AZO interface. Moth eye textured coatings have been extensively reported as antireflective coatings on glass and polymeric substrates.[11–14]

EXPERIMENTAL

(1) *NIL*

The moth-eye nanostructures were applied through NIL. The process used consisted of two main steps: preparation of the replica and structuring of the resist.[14] To prepare the replica, a first layer of hard PDMS was applied on top of the mold, followed by a second layer of soft PDMS, according to the procedure described by Schmid *et al.*[15] The Kriya SPF1439-A3 transparent UV curable resist was applied with a 30 μm Bird applicator and directly imprinted by gently pressing the replica into the wet coating. Drying of the resist occurred overnight at room temperature. After UV curing of the resist, the replica was removed from the substrate.

(2) *Manufacturing of CIGS solar cells*

CIGS cells were fabricated on 10 x 10 cm^2 soda lime glass substrates.[16] After glass cleaning a 350 nm thick Mo was sputtered with a 1 kW DC Argon plasma from a 12 x 42,5 cm^2 planar rectangular target. Subsequently, the CIGS absorber was co-evaporated from 4 different elemental sources following a 3-stage-like process where substrate temperature was kept constant at 550°C. Absorber thickness was adjusted by changing the deposition time of the first stage. Immediately after CIGS evaporation a 50 nm CdS buffer layer was deposited with a chemical bath technique. Finally, a 50 nm intrinsic ZnO/230 nm AZO window layer was sputtered in the same tool as the Mo to complete the cell stack. A Cu grid was then applied through thermal evaporation and the 10 x 10 cm^2 substrate was scribed into 162 individual 5 x 10 mm^2 cells.

(3) *Analyses of CIGS solar cells*

(I,V)-curves of the cells were measured under standard AM1,5 conditions with a class AAA Trisol solar simulator operating under 1 sun. (I,V)-measurements were performed before and after application of the moth-eye textured resist. Spectral response was measured in the wavelength range between 300 and 1100 nm with a spectral resolution of 10 nm. A commercial spectral response set-up by Optosolar (SR300) with a 250 W xenon lamp and a Jobin Yvon iHR320 monochromator was used. The measurement is performed with a 1 mm beam spot on the active area of the cell. The system was calibrated with a Thorlabs S120VC crystalline silicon reference solar cell. Calculation of the external quantum efficiency (EQE) was performed with the measured spectral response data

and AM1,5G spectrum according to IEC60904-3, using the relation

$$EQE = \frac{SR}{\lambda} * \frac{hc}{e}$$

With SR for spectral response, λ for wavelength, h is the Planck constant ($6.626 \cdot 10^{-34}$ J·s), c is the speed of light in vacuum ($3.0 \cdot 10^{8}$ m·s^{-1}) and e is the elementary charge ($1.602 \cdot 10^{-19}$ C).

RESULTS AND DISCUSSION

The refractive index of the sputtered AZO layer, which is applied as transparent conductor in the CIGS cells used in this study, was determined *via* ellipsometry (FIG. 1). The refractive index of this layer at a wavelength of 633 nm is 1.913. As resist for UV NIL, we selected Kriya SPF1439-A3, a polymeric resist filled with titanium dioxide nanoparticles. Although the refractive index of this resist – 1.792 at 633 nm wavelength – differs significantly from the refractive index of sputtered AZO, it is sufficiently similar to avoid large optical losses at the resist-AZO interface. The expected reflection at that interface is 0.106% at 633 nm.

As suitable texture for the resist layer, we selected a moth-eye type texture to reduce the reflection at the interface resist-air.[14,17–19] To apply the moth-eye texture, we used the HT-AR-02 mold from NILT. This mold has following specifications: the grating is a hexagonal array with a pitch of 300 nm and an average height of 350 nm. We replicated this mold in PDMS. The PDMS replica was used to texture the resist using conventional wafer-by-wafer UV NIL. Using AFM analysis, we demonstrated that the surface texture of the mold was well replicated in the PDMS replica, and that the surface texture of the PDMS replica was well replicated in the resist layer (FIG. 2).

As demonstrated in FIG. 2, the pitch of the texture in HT-AR-02, the PDMS replica and the imprint in Kriya SPF1439-A3 was identical (300 nm). In the replication steps mold to replica and replica to resist, the texture is well replicated; the average height only slightly decreases from 327 nm (HT-AR-02 mold) to 301 nm (imprint in Kriya SPF1439-A3).

To evaluate the change in surface reflection upon use of the resist layer, we applied a 2.2 μm thick non-textured resist layer on a 0.28 μm thick AZO layer on glass, and a moth-eye textured resist layer with a residual layer thickness of 1.8 μm. We performed reflection and absorption measurements under near normal angle for the wavelength regime 300-1100 nm of following layer stacks: glass-AZO, glass-AZO-non-textured resist, and glass-AZO-textured resist (FIG. 3).

As demonstrated in FIG. 3(a), the average reflection of a 0.28 μm thick AZO on glass in the wavelength regime from 300 nm to 1100 nm is 14.5%. The strong oscillation is caused by the coherent light propagation through the thin AZO layer. This means that constructive and destructive interference occurs with varying wavelength of the incident light. In the wavelength regime between 300 nm and 500 nm, strong absorption is observed (46.7%, FIG. 3(b)).

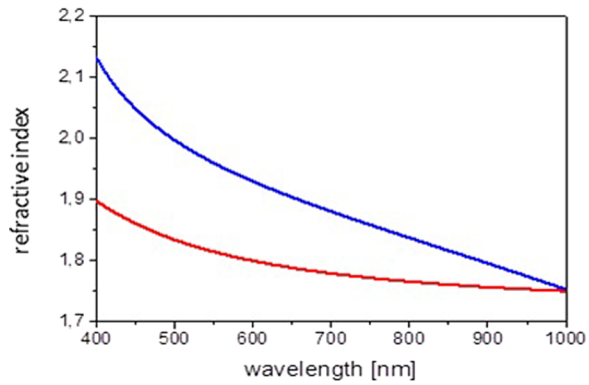

FIG. 1. Refractive index of AZO (blue) and Kriya SPF1439-A3 (red) in the wavelength regime 400 – 1000 nm determined *via* ellipsometry.

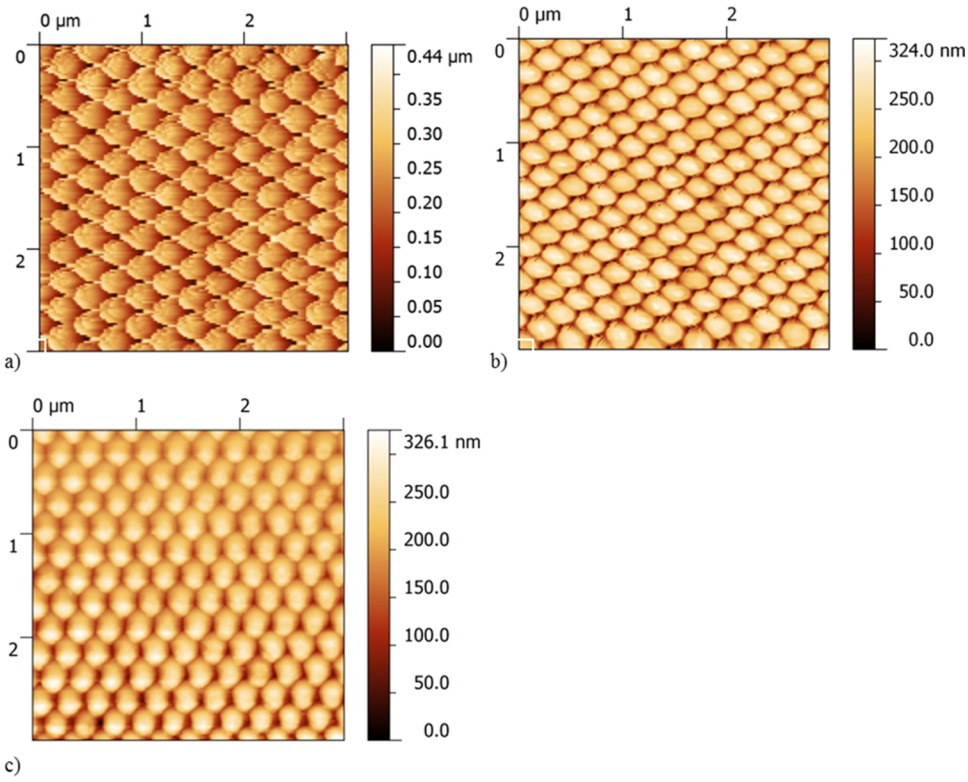

FIG. 2. AFM images of a) HT-AR-02 mold, b) h-PDMS replica, c) imprint in Kriya SPF1439-A3 on top of AZO.

Upon application of a 2.2 µm thick non-textured layer of Kriya SPF1439-A3, the average reflection in the wavelength regime from 300 nm to 1100 nm decreased to 13.3% (FIG. 3(a)). The absorption in the wavelength regime between 300 nm and 500 nm increased to 49.1% (FIG. 3(b)). The oscillation observed for the AZO layer is largely reduced by the thick resist layer, since light propagation becomes (partially) incoherent.

Upon application of a moth-eye textured layer of Kriya SPF1439-A3, the average reflection decreases to 5.7% in the wavelength regime from 300 nm to 1100 nm (FIG. 3(a)). The average absorption in the regime between 300 nm and 500 nm is 58.1%. *Ergo*, the moth-eye textured resist on AZO reduces the overall reflection in the range between 300 nm and 1100 nm by 8.8%. In the regime between 500 and 1000 nm, the reflection is reduced by 7.0%.

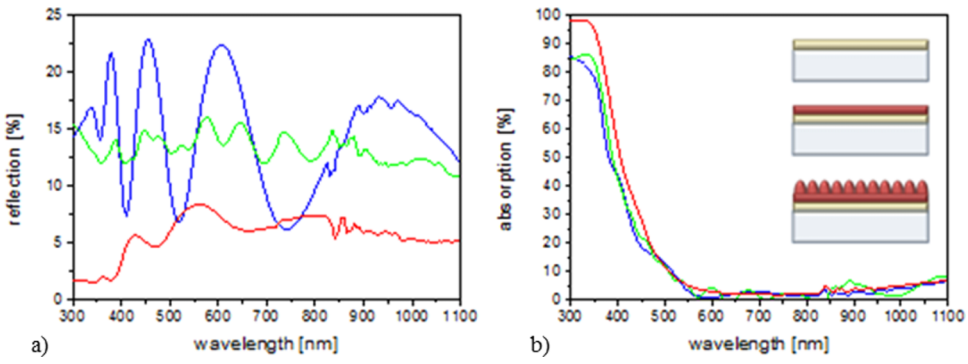

FIG. 3. (a) Reflection and (b) absorption of AZO on glass (blue), AZO on glass, coated with non-textured resist (green), and AZO on glass, coated with textured resist (red) in the wavelength regime 300 – 1100 nm. A schematic representation is included.

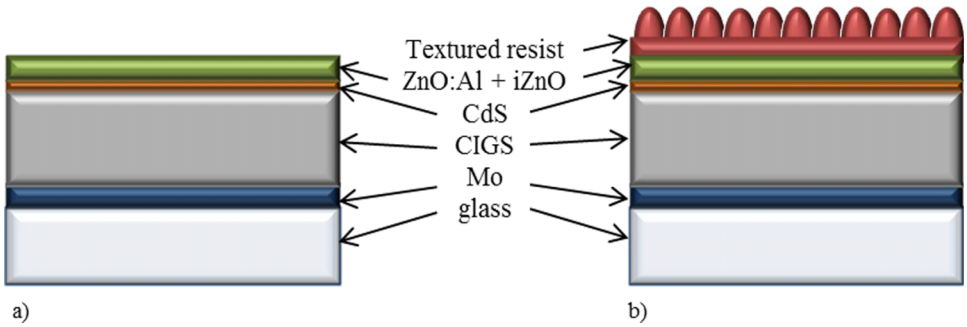

FIG. 4. Schematic representation of a CIGS solar cell (a) without and (b) with textured resist.

To validate the effect of this reduction in reflection, we manufactured CIGS solar cells as follows: first, a 0.35 μm thick Mo layer was applied to the glass substrate through sputtering, followed by the deposition of the CIGS absorber layer in a co-evaporation process. Subsequently, a 50 nm CdS buffer layer was applied in a wet-chemical deposition process, followed by deposition of a 50 nm thick intrinsic ZnO and 230 nm thick AZO layer through sputtering. Then, the Kriya SPF1439-A3 resist was applied and textured using UV NIL (*vide supra*). Schematic representations of a CIGS cell without and with textured resist are presented in FIG. 4.

As initial system, we studied a CIGS solar cell as described above with d_{CIGS} = 1.00 μm. The layer stack was deposited on a 10 x 10 cm^2 glass substrate. Subsequently, the substrate was divided into 162 cells of 0.5 cm^2, on which copper electrodes were deposited. Sixteen cells were coated with Kriya SPF1439-A3 and textured using NIL.

(I,V)-curves for a cell with 1.00 μm thick absorber layer without and with textured resist confirm that both cells are of high quality. Sixteen cells were analyzed before and after application of moth-eye textured Kriya SPF1439-A3. The cells without resist show an open-circuit voltage (V_{oc}) of 0.61 ± 0.01 V, an J_{sc} of 25.38 ± 0.30 mA·cm^{-2}, a fill factor (*FF*) of 71.5 ± 1.8% and an efficiency of 11.03 ± 0.42%. After coating with Kriya SPF1439-A3 and subsequent texturing *via* NIL, we obtained cells with a V_{oc} of 0.60 ± 0.01, an J_{sc} of 28.07 ± 0.44, a *FF* of 70.3 ± 1.5% and an efficiency of 11.93 ± 0.51%. Hence, the textured resist causes a relative increase in J_{sc} of 10.6% and in efficiency of 8.2%.

To validate that the origin of this increase in J_{sc} and cell efficiency is related to the reduction in reflection (R) caused by the nano-textured resist, we measured the reflection and determined the external quantum efficiency (EQE) of the cells before and after application of the moth-eye textured Kriya SPF1439-A3 (FIG. 5).

In the wavelength regime below 500 nm, most of the light entering the solar cell is absorbed by the AZO and CdS layers. Hence, the nanotextured resist does not have any significant influence

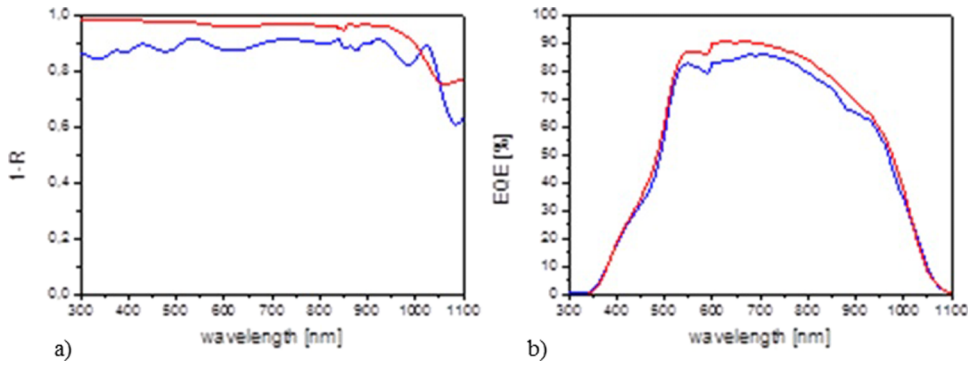

FIG. 5. (a) (1-R) and (b) EQE curves of CIGS solar cell with absorber layer thickness of 1 μm without (blue) and with (red) textured resist.

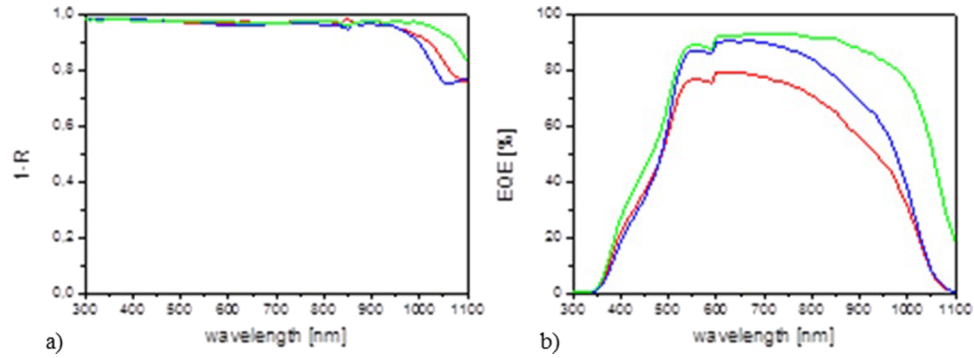

FIG. 6. (a) (1-R) and (b) EQE curve of CIGS solar cell (d_{CIGS} = 0.85μm (red), 1.00 μm (blue) and 2.00 μm (green)) with moth-eye textured resist.

on the EQE in this wavelength regime. In the regime between 500 nm and 1000 nm, the increase of 7.5% in (1-R) through use of the moth-eye textured resist causes an increase in EQE of 4.4%. At higher wavelengths, (1-R) is not increased through use of the moth-eye textured resist, and consequently the EQE is not increased.

When comparing (1-R) and EQE of CIGS cells with an absorber layer thickness of 0.85 μm, 1.00 μm and 2.00 μm and moth-eye textured resist, the expected optical losses for cells with an absorber layer thickness less than 2.00 μm are observed (FIG. 6).[10] For the CIGS cells with 1.00 μm and 0.85 μm absorber layer thickness, similar optical losses occur in the wavelength regime above 950 nm caused by incomplete absorption of the light in the thinner absorber layer. These optical losses are reflected in the EQE.

As demonstrated in Table I, the J_{sc} increases upon integration of the moth-eye textured Kriya SPF1439-A3 for all three absorber layer thicknesses: by 1.56 mA·cm^{-2} (6.8%) for d_{CIGS} = 0.85 μm, 2.69 mA·cm^{-2} (10.6%) for d_{CIGS} = 1.00 μm and 1.36 mA·cm^{-2} (4.3%) for d_{CIGS} = 2.00 μm. The fill factor slightly decreases upon integration of the moth-eye textured resist (max. 1.7% decrease). The cell efficiency increases for all three absorber layer thicknesses: by 4.2% for d_{CIGS} = 0.85 μm, 8.2% for d_{CIGS} = 1.00 μm and 5.5% for d_{CIGS} = 2.00 μm. On average, J_{sc} increases by 7.2%, which matches the average reduction in reflection of 7.0% between 500 and 1000 nm. The average relative increase in efficiency is slightly lower (6.0%). No trend towards a larger relative increase in J_{sc} with decreasing d_{CIGS} was observed; we did not observe any increase in J_{sc} based on an increased photon path length. The diffraction effect caused by the moth-eye structure in the resist layer does not affect the absorption in the CIGS layer. To make the diffraction of the sub-wavelength patterning effective, the pattern has to be either in direct contact with or at maximum at 100 nm distance of the active layer. Given the i-ZnO/AZO layer thickness of 280 nm, this cannot be achieved in a CIGS cell stack. Latter is in agreement with the results from optical simulation studies reported by Čampa *et al.*[20]

TABLE I. Efficiency of CIGS solar cell with absorber layer thickness of 0.85 μm, 1.00 μm and 2.00 μm with and without textured resist.

		V_{oc} [V]		J_{sc} [mA·cm^{-2}]		*FF* [%]		*Efficiency* [%]	
d_{CIGS} [μm]	*Number of cells*	Before	After	Before	After	Before	After	Before	After
0.85	10	0.64 ± 0.01	0.64 ± 0.01	22.98 ± 0.94	24.54 ± 1.13	71.6 ± 1.9	69.9 ± 2.2	10.49 ± 0.54	10.93 ± 0.66
1.00	16	0.61 ± 0.01	0.60 ± 0.01	25.38 ± 0.30	28.07 ± 0.44	71.5 ± 1.8	70.3 ± 1.5	11.03 ± 0.42	11.93 ± 0.51
2.00	13	0.65 ± 0.02	0.66 ± 0.02	31.92 ± 0.58	33.28 ± 1.11	70.9 ± 1.9	70.8 ± 1.9	14.66 ± 0.53	15.47 ± 0.49

CONCLUSIONS

In conclusion, we have demonstrated that the integration of a moth-eye textured resist layer with a refractive index sufficiently close to AZO to avoid large optical losses at the interface resist-AZO (n_{resist} = 1.792 *vs.* n_{AZO} = 1.913 at 633 nm), results in an increase in J_{sc} and cell efficiency for CIGS cells with absorber layer thicknesses of 0.85 μm, 1.00 μm and 2.00 μm. On average, J_{sc} increases by 7.2%, which matches the average reduction in reflection of 7.0%. The average relative increase in efficiency is slightly lower (6.0%). No trend towards a larger relative increase in J_{sc} with decreasing d_{CIGS} was observed. The observed increase in J_{sc} and cell efficiency upon integration of the moth-eye textured resist can be fully explained by the reduction in reflection caused by the moth-eye texture, which is in line with the results from optical simulation studies reported by Čampa *et al.*[20]

ACKNOWLEDGMENTS

The authors gratefully acknowledge K. Bakker (ECN, Eindhoven, The Netherlands) for help with spectral response measurements, H. Rooms (TNO) for ellipsometry measurements and M. Saalmink (TNO) for AFM characterization of the nanotextured surfaces. We thank RAAK/SIA for financial support in the RAAK Pro project "UV absorberende nanodelen."

[1] J. Krč, M. Zeman, O. Kluth, F. Smole, and M. Topič, Thin Solid Films **426**, 296 (2003).
[2] V. Jovanov, X. Xu, S. Shrestha, M. Schulte, J. Hüpkes, M. Zeman, and D. Knipp, Sol. Energ. Mat. Sol. C. **112**, 182 (2013).
[3] J. Müller, B. Rech, J. Springer, and M. Vanecek, Sol. Energy **77**, 917 (2004).
[4] M. Zeman, O. Isabella, S. Solntsev, and K. Jäger, Sol. Energ. Mat. Sol. C. **119**, 94 (2013).
[5] C. Battaglia, C.-M. Hsu, K. Söderström, J. Escarré, F.-J. Haug, M. Charrière, M. Boccard, M. Despeisse, D. T. L. Alexander, M. Cantoni, Y. Ciu, and C. Ballif, ACS Nano **6**, 2790 (2012).
[6] W. Beyer, J. Hüpkes, and H. Stiebig, Thin Solid Films **516**, 147 (2007).
[7] A. P. Vasudev, J. A. Schuller, and M. L. Brongersma, Opt. Express **20**, A385 (2012).
[8] O. Isabella, J. Krč, and M. Zeman, Appl. Phys. Lett. **97**, 101106 (2010).
[9] R. W. Miles, G. Zoppi, and I. Forbes, Mater. Today **10**, 20 (2007).
[10] M. Xu, A. J. H. Wachters, J. van Deelen, M. C. M. Mourad, and P. J. P. Buskens, Opt. Express **22**, A425 (2014).
[11] J. H. Shin, K. S. Han, and H. Lee, Prog. Photovolt: Res Appl. **19**, 339 (2011).
[12] T. Senn, O. Kutz, C. Weniger, J. Li, M. Schoengen, H. Löchel, J. Wolf, P. Göttert, and B. Löchel, J. Vac. Sci. Technol. B **29**, 061601 (2011).
[13] S. Y. Kuo, M. Y. Hsieh, H. V. Han, F. I. Lai, T. Y. Chuang, P. Yu, C. C. Lin, and H. C. Kuo, Optics Express **22**(3), 2860 (2014).
[14] M. Burghoorn, D. Roosen-Melsen, J. de Riet, S. Sabik, Z. Vroon, I. Yakimets, and P. Buskens, Materials **6**, 3710 (2013).
[15] H. Schmid and B. Michel, Macromolecules **33**, 3042 (2000).
[16] A. Kuypers, R. Knaapen, M. Theelen, M. Meuris, M. van der Vleuten, and W. Zijlmans, Photovoltaics International **20**, 63 (2013).
[17] K. Forberich, G. Dennler, M. C. Scharber, K. Hingerl, T. Fromherz, and C. J. Brabec, Thin Solid Films **516**, 7167 (2008).
[18] K.-S. Han, J.-H. Shin, W.-Y. Yoon, and H. Lee, Sol. Energ. Mat. Sol. C. **95**, 288 (2011).
[19] N. C. Linn, C.-H. Sun, P. Jiang, and B. Jiang, Appl. Phys. Lett. **91**, 101108 (2007).
[20] A. Čampa, J. Krč, J. Malström, M. Edoff, F. Smole, and M. Topič, Thin Solid Films **515**, 5968 (2007).